EVS27
Barcelona, Spain, November 17-20, 2013

Detection of Electric Arcs in Large Batteries

V. Cattin[1], P. Perichon[1], J. Dahmani[2], B. Schwartzmann[1], V. Heiries[1]
[1]*CEA LETI/LITEN, Minatec, Grenoble, France, viviane.cattin@cea.fr, pierre.perichon@cea.fr, Benjamin.schwartzmann@cea.fr , vincent.heiries@cea.fr*
[2]*Grenoble INP, GIPSA-lab, St Martin d'Hères, France*

Abstract

This paper addresses the precocious detection of electric arcs in an electric vehicle battery generated by a connector fault. The detection principle is based on the acoustic emission of the arc. First, the identification of the electric arc acoustic signature as well as disturbances in the environment of detection has been realized. Subsequently, we have been focused on the propagation of acoustic waves emitted by the arc in the confined environment of the battery. We proposed a detection method based on correlation whose performance was evaluated. Finally, a localization system based on signal time-difference-of-arrival estimation and triangulation is described and assessed. A demonstrator has been developed and validates the detection performance.

Keywords: electric arc, battery monitoring, acoustic signal processing

1 Introduction

The battery of an EV is made of several modules and each module consists of several battery cells arranged in series and in parallels. This type of arrangement leads to a high number of internal connections. The connections between these cells may be damaged or broken due to the aging of materials, or other external factors (shocks and vibrations in the vehicle). A break at the connection may cause electric arcs that can be maintained because of DC current flowing into the battery. Thus, these arcs can cause overheating and even thermal runaway in the battery which can lead to dangerous fires. Thereby the aim of our study is to detect these arcs from their beginning and prevent possible thermal runaway. Because of the many disturbing transient signals present on the voltage and the current measurements made on the battery, we propose an innovative method based on the acoustic emission of electric arcs. Firstly, the arc acoustic emission nature is discussed theoretically and experimentally. Secondly, the acoustic environment in the framework of our vehicle application has been assessed. The different interfering signals have been listed and characterized. Thirdly, an electric arc detection method is proposed and thoroughly evaluated. Further on, a localization system is studied. Finally, the demonstrator realized to implement the detection method and to validate it is presented.

2 Acoustic study of the electric arc

In this section, we propose a theoretical and experimental study of electric arcs.

2.1 Theoretical study

The physical process that starts an arc in the battery is by contact. An electric arc can be produced when two contacts initially driven by a current are separated. The conduction is then maintained by an electric discharge that begins in the space between electrodes. A battery contains several connections between cells, which are likely

to have defects and then cause arcs. The minimum voltage needed in order to maintain the arc is around 15-20V. Below this value, the space charge area near the electrodes becomes insulating and then the arc stops.
An electric arc generates acoustic waves whose amplitude can vary depending on several parameters. The equation of the wave in the plasma is [1] :

$$\nabla^2 p = \frac{1}{c^2}\frac{\partial^2 p}{\partial t^2} - \frac{(\gamma - 1)}{c^2}\frac{\partial H}{\partial t} + divF_1 - \frac{\partial Q}{\partial t} \quad (1)$$

where p is the perturbation of the pressure, c is the speed of sound, γ is the adiabatic compression coefficient, H is the first-order perturbation of any quantity of energy delivered per second per unit volume of gas, and Q is the quantity perturbed to first order of Q_0 which is the mass of neutral particles received per second per volume unit.
Equation (1) can be simplified to:

$$\nabla^2 p - \frac{1}{c^2}\frac{\partial^2 p}{\partial t^2} = -S(r,t) \quad (2)$$

where $S(r,t)$ is the term for the source.
The amplitude A of the acoustic wave at a given point is proportional to $\frac{\partial W}{\partial t}$, where $\frac{\partial W}{\partial t}$ is the electric power transferred to the arc. After simplification, the amplitude can be written as:

$$A = \alpha \frac{(\gamma - 1)}{c^2}\frac{\partial W}{\partial t} \quad (3)$$

where α is the coefficient inversely proportional to the temperature of the arc.

We can notice here that the parameters of the arc have only influence on the magnitude of the acoustic signal but not on its spectral signature. This property will be useful to choose the detection method.

2.2 Experimental study

In this section, we present acoustic signatures typical of experimental arcing. When an arc due to a fault connection is produced in a battery, it has a voltage of the order of fifty volts (depends on the connectors spacing) for an hundred amperes. In order to experimentally reproduce this phenomenon in a secure environment we have designed a specific RLC circuit. Melting a fuse wire located between two electrodes creates the arc. We sized the various components (R, L, and C) in order to obtain the desired voltage, current and arc duration.
On figure 1 we plot the time acoustic signal produced by a fuse arc and its frequency spectrum. We used a piezoelectric sensor from Euro Physical Acoustics (EPA) SA, which frequency band reaches 1MHz.

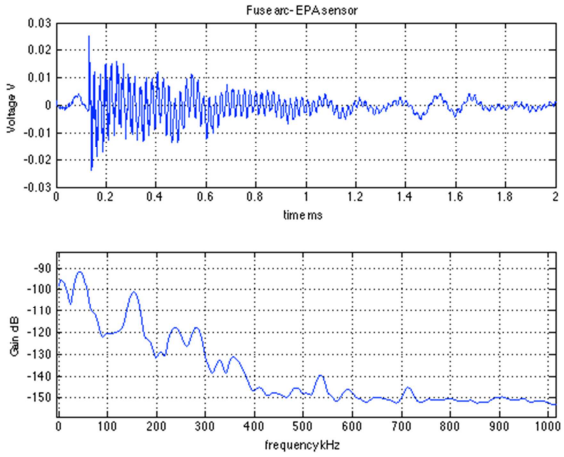

Figure 1: Time and frequency signatures of a fuse arc measured with an EPA sensor.

In the time area, the signal extends over several milliseconds with a decreasing envelope. This shape recalls the impulse response of a filter. In the frequency area, there is a greater power at low frequencies, especially in the audible area (which is perceptible to the ear). This spectrum shows resonances around 10 kHz, 40 kHz and 150 kHz.
We plot on figure 2 results obtained for the same arc with a sensor from Avisoft Bioacoustics, which is characterized by a flat frequency response up to 200 kHz.

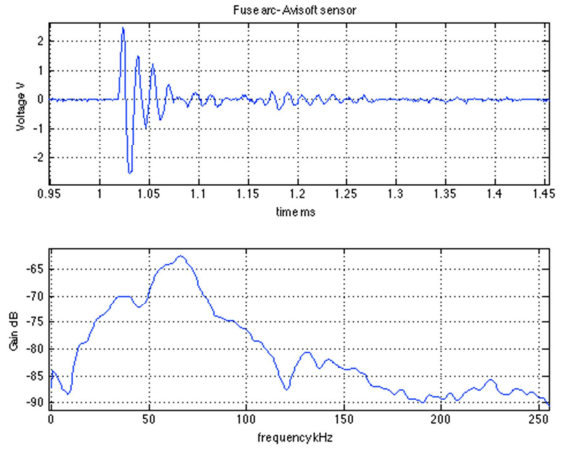

Figure 2: time and frequency signatures of a fuse arc measured with an Avisoft sensor.

The transient signature of the fuse arc is this time very short, on the order of 0.1 ms. In the frequency area, the main lobe extends from DC to 150 kHz. Any specific frequency appears in this second spectrum.
Similar experimental measurements performed with other types of arcs confirm these observations. The specificity of the acoustic arc signal is rather in the time area: it is characterized by a transient signature with a decreasing envelope. Apart single resonances due to the responses of the sensors, no specific frequency can be identified on arc spectra.
We studied the influence of various parameters of the arc on the resulting acoustic signal. It was found that the greater the distance between the electrodes (and therefore the power of the arc), the stronger the amplitude of the signal becomes. We also note that the power of the arc has no influence on the spectral distribution of the acoustic signal: no frequency component stands out from the overall spectrum.
These results are coherent with what is described by the theoretical relationship (equation (4)):

$$A = k\frac{\partial V(t).I(t)}{\partial t} \text{ with } k = \alpha\frac{(\gamma-1)}{c^2} \quad (4)$$

Indeed, the greater the distance between the electrodes, the higher the dielectric breakdown voltage becomes. This implies a more powerful sound.
We conclude from this experimental study that there is no specific frequency signature of an electric arc signal. The spectrum extends over the whole frequency band of ultrasound (20 kHz to 200 kHz), with resonances due to the responses of the sensors. However, in the time area, we note that a signal from an arc is very specific: it is characterized by one or more oscillations (depending on the transducer used) with an amortized envelope. This will guide us to build the detector of the arc based mainly on the time signature.

3 Acoustic study of vehicle noises

To achieve the design of a detector, it is necessary to determine the signature of the signal to be detected but also the acoustic noises of the environment. We have therefore conducted experiments on an EV to characterize the acoustic disturbances produced by the different components of the system.

These measurements are also used to evaluate the performance of the detector: real disturbances are added in simulations to study the robustness of the detector in conditions close to reality. The following table summarizes the main disturbances measured (table 1):

Table1: summary of the acoustic disturbances in the car (position of the sensor, event, main frequency band covered by the spectrum).

Position	Event	Frequency band of the spectrum (kHz)
Blinking box	Blinker	10 → 95
Close to the handle	Car door slam	5 → 75
Next to battery	Normal driving	0 → 35
	Acceleration	0 → 60
	Brake	0 → 45
Motor Normal	Normal driving	0 → 85
	Acceleration	0 → 40
	Brake	0 → 250

In the case of the motor, the blinker, and the door, the acoustic sources are easily identified. However in the case of the battery, the sources of the measured signals are unknown, so we can only assume that they come from vehicle vibration, bearings, wheel noise, or other vibration phenomena present in the car. We plot on figure 3 two examples of time signals of disturbances to illustrate some shapes.

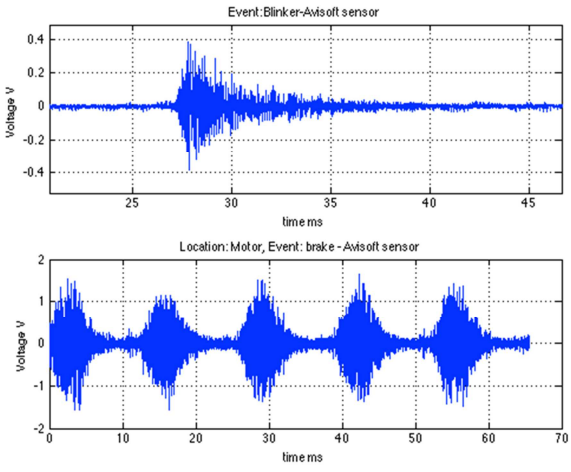

Figure 3: examples of signals of acoustic disturbances in the EV (above: blinker signal, below: brake signal).

It is clear from these results that ultrasound acoustic emission is present at various locations in

the vehicle, and these disturbances can induce false alarms. Indeed, most of the spectra of the recorded signals overlap that of the arc. So a processing based only on a simple frequency filter is not suitable. However, time signals of the disturbances are very different from the signature of an arc. Some consist of repeating patterns, while other present unamortized envelopes.

4 Acoustic propagation in the battery environment

The propagation of ultrasonic waves in the environment of a battery is an important issue in the context of this study. Therefore understanding the influence of this environment on the acoustic wave will help us to fully characterize the signal to be detected. The design of a battery cell can be cylindrical or prismatic. In some cases, connectors are located on the same face and are more accessible, so the propagation of the acoustic signal is free and detection is easy. We thus focus on cylindrical battery cells with terminal connection geometrically opposite, which give a more complex problem of detection. Indeed multiple connections between cylindrical cells are masked and the propagation of the acoustic wave is complex with a lot of phenomena (refraction, reflection, scattering) on the cells walls and packaging which rapidly reduces the waves or creates resonances.

First of all it is important to understand how the ultrasonic wave is generated. The electric arc is produced by breaking a connection between two cells. The plasma is created in the air and therefore the majority of the power of the wave produced by the arc is released into the air. A small portion of the wave created at the arc feet will propagate into connectors and cells, but this part is negligible compared to the wave propagated in the air. Indeed, the acoustic impedance of a cell is very high (Zcell=4, 5×106Kg.m−2.s−1) compared to that of air (Zair=440Kg.m−2.s−1), and the transmission coefficient in the material is very low (about 0.1% for an incidence angle of 90°). So the acoustic power of the wave coming from the air and propagated within the material is negligible. We can thus consider that the main propagation of the acoustic wave produced by the electric arc takes place in the air. Therefore the sensors used for the detection must be microphones that present an excellent coupling with the air.

Secondly to experimentally verify the above assumptions, we produced arcs at a connection on a set of cells and we measured the acoustical signal which has propagated through cells (by reflexion on the cell wall or transmission into the cell) and in the air. Results (figure 4) show that almost no propagation takes place in the material. Main waves received by the sensors come from the propagation in the air.
More precisely, the blue sensor located in the air received the highest signal of the arc whereas the red and green ones coupled with the faces of the cells recorded very small signals close to the noise.

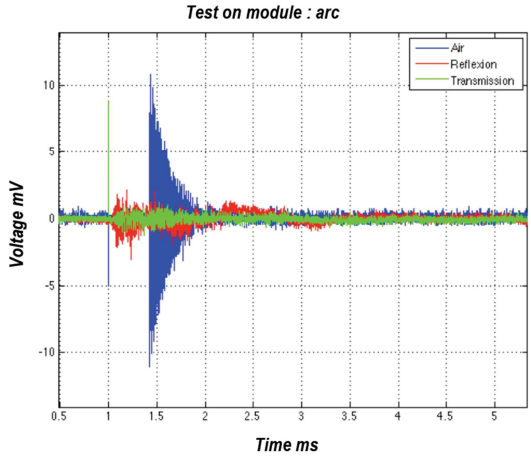

Figure 4: acoustic record of an arc on a set of battery cells (blue : propagation in air, red : propagation by reflection on cells, green : propagation trough cells)

5 Detection method

The problem consists in detecting the presence of an event in a noisy environment [2]. In binary detection theory, the problem is reduced to decide if a specific signal is present or not in the noise. Each of these situations can be written as a hypothesis, denoted H0 or H1:

$$\begin{cases} H_0 : x(t) = b(t) \\ H_1 : x(t) = s(t) + b(t) \end{cases} \quad (5)$$

We denote by $x(t)$ the observation signal, $s(t)$ is the signal to be detected, and $b(t)$ is the additive noise. We usually associate to a detection problem a function $d(x)$ of the observation x called detection test. This function takes binary values giving the information of the decision to choose; $d(x) = 1 \Rightarrow$ we decide H_1 and $d(x) = 0 \Rightarrow$ we decide H_0.

Several detection methods exist and each has its own performance which depends on the conditions of detection: noise characteristics or the signature to detect. Our detection problem consists in detecting a known waveform in a recorded signal. As proved in the first part of this paper, it is better in our case to exploit the time shape of the signal to realize the detection.

Two indicators usually determine the quality of a detector [3]: the probabilities of correct detection P_d and false alarm P_{fa}. The receiver operating characteristic curves (ROC) give the evolution of P_d as a function of P_{fa} for a given signal to noise ratio (SNR). When these densities are not known, which is often the case in practice, one technique is to plot experimental or simulated curves, what we will do in our case. The method consists in using a test signal made of the signal to be detected, some noise and some disturbances specific from the environment. In our case, the test signal is built from an arc signal with white Gaussian noise and several disturbances recorded in the EV. The fine locations of the arc and disturbances in the signal are known, so after applying the detection algorithm on the test signal we are able to calculate the probabilities of correct detection (response to the arc) and false alarm (response to disturbances or noise). Figure 5 shows an example of such test signal.

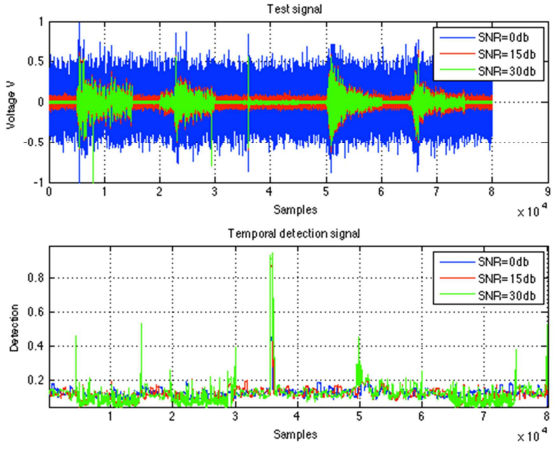

Figure 5: examples of test signal (above: test signals with three level of SNR, below: detector output for the three cases).

The studied detection method consists in measuring the similarity between the signal received by the sensor and a model of the arc. So the first step is to model the arc signal: we used an ARMA process since it is well suited to describe oscillating signals amortized. We then detect the presence of the arc by correlating the time signal measured by the sensors with this model. To apply this method, we cut the signal with a sliding window, and for each position of the window we compute a normalized correlation coefficient between the model and the signal contained in the window. Detection is then performed by applying a threshold on the time detection curve thus obtained. This threshold is selected in order to obtain the desired probabilities of good detection and false alarm. We plot on figure 6 an example of a simulated signal including two arcs and other disturbances measured on the EV. We apply the above detection method on this signal and the time detection curve is computed.

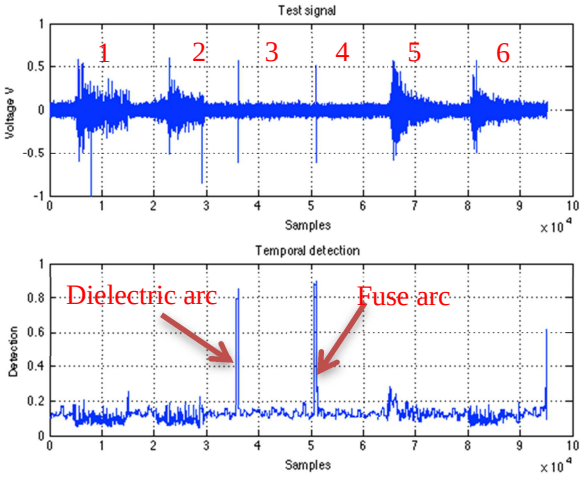

Figure 6: test signal (above) and normalized time detection curve (below) for the detection by correlation.

Pattern numbered from 1 to 5 in the test signal correspond respectively to the signals of: brake, acceleration, dielectric arc, fuse arc, turn signal, and banging of the door. From the time detection curve, the binary information of the detection is obtained by selecting a threshold between 0 and 1. We can clearly distinguish the responses of the detector to the arc signals. We present in figure 7 the ROC curve obtained with the detection by correlation.

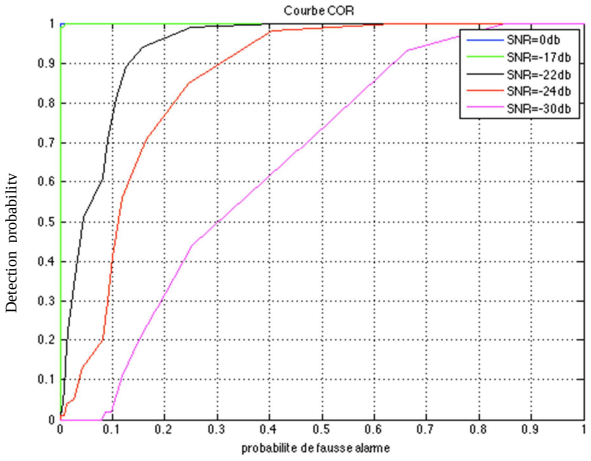

Figure 7: ROC curves for the detection by correlation for several SNR.

This method of detection by correlation is very robust, indeed for smaller SNR the probabilities of correct detection and false alarm are both excellent. However it requires a fine knowledge of the time signature of the arc. As the model is sensitive to the properties of the sensor (in particular its resonances), it must be adjusted each time we change the sensor.

Another arc detection method based on higher order statistics has been assessed in a previous study ([4]), but the performance reached were lower compared to the results obtained using the correlation method.

6 Localization of the arc

In order to increase the efficiency during maintenance and fixing of the battery after the electric arc outbreak detection, it could be highly valuable to get the arc localization information.
In this perspective, a localization method based on a typical triangulation process has been studied. We have focused our work on a two dimension plan localization problem.

6.1 General principle

Three acoustic sensors with known exact positions are arranged at the edge of the area of interest. The acoustic signal emitted by the arc is received at the three sensors, and via a typical Time Difference Of Arrival (TDOA) determination the position of the electric arc is computed.

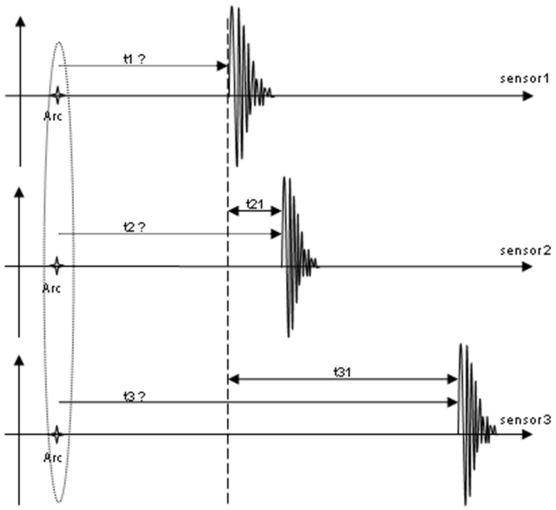

Figure 8: arc acoustic signal in the three sensors' timescale

This three sensors system is supposed synchronous with no bias between the sensors timescale. As illustrated on Figure 8, one sensor, e.g. sensor 1, is defined as the reference, and the difference of acoustic signals time-of-arrival t_{21} and t_{31} is evaluated. These time difference measurements are expressed as follows:

$$t_{21} = t_2 - t_1$$
$$t_{31} = t_3 - t_1 \quad (6)$$

The associated distances are defined as follow, v_s being the speed of sound in the air:

$$d_{21} = v_s \cdot t_{21}$$
$$d_{31} = v_s \cdot t_{31} \quad (7)$$

These measured distances are linked to the arc coordinates (x_A, y_A) and the sensors coordinates (x_{Si}, y_{Si}), with $(i = 2,3)$, through the equation (8) :

$$d_{21} = \sqrt{(x_A - x_{S2})^2 - (y_A - y_{S2})^2} - \sqrt{(x_A - x_{S1})^2 - (y_A - y_{S1})^2}$$
$$d_{31} = \sqrt{(x_A - x_{S3})^2 - (y_A - y_{S3})^2} - \sqrt{(x_A - x_{S1})^2 - (y_A - y_{S1})^2} \quad (8)$$

The estimation of the arc position $(\widehat{x_A, y_A})$ from the inversion of equation (8) is performed off-line by using a Levenberg-Marquardt least square algorithm.
Obviously, several errors may affect the acoustic sensors and have been modelled on the distance values by an additive bias during simulations.

6.2 Analysis of the acoustic sensors arrangement issue

In order to optimize the position estimation accuracy, the sensors used need to be arranged in the best possible configuration. A study on the impact of the sensors configuration on the position estimation accuracy has been herein carried out.

A 100 mm side square in a two dimensions plan is defined into which electric arcs are simulated with randomly distributed positions. The arc localization is done through the method described in the previous paragraph. The three acoustic sensors are placed around this square, and several sensors positions are tested (65 different configurations). For each sensors positions configuration, 50 arcs are simulated and the localization estimation accuracy is analysed. On Figure 9, the root mean square error (RMSE) of the arc position estimation for a number of sensors location configurations is plotted. This resulting RMSE is comprised between 2.2 mm for the best configuration and 16.1 mm for the worst configuration. This result highlights the interest of choosing a correct setting for the sensors although centimetre accuracy is sufficient for battery reparation.

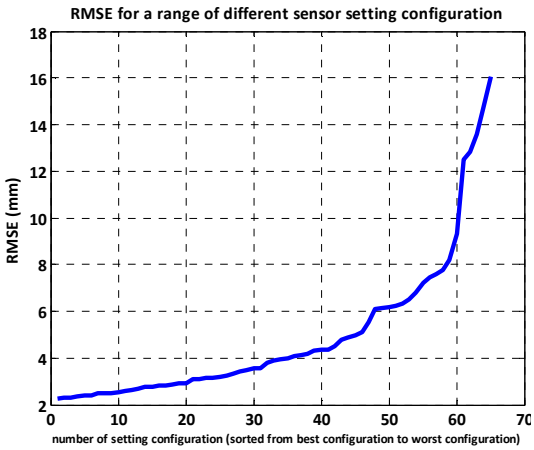

Figure 9: influence of the sensors location setting on the arc localization precision

The Figure 10 displays the arc localization precision obtained by the estimation onto the plan square defined for the simulations for four different configurations of sensors represented on the figure by black squares. The colorbar scales the estimation precision in millimetre. This figure illustrates the dilution of precision of the estimation which is a consequence of the acoustic sensors coverage of the area of interest. The larger area delimited by the sensors, the larger optimum estimation accuracy area extends.

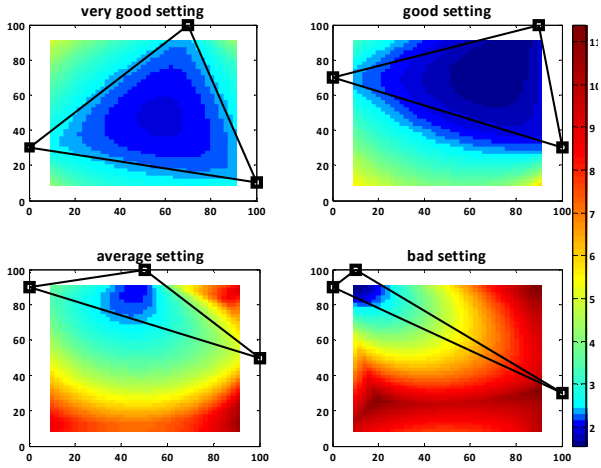

Figure 10: influence of the sensors coverage

Then, these four different settings have been hold for the simulation. An electric arc is generated in three zones: inside, outside and close to the acoustic sensor coverage area. The result in terms of arc localization accuracy is showed on Figure 11. The coloured curves pictured on this figure represents the cost function to be minimized in the TDOA localization inversion problem.

It can be noticed that the localization accuracy decreases as the arc is moved away from the sensors coverage area, and that the localization performance is strongly impacted by the sensors configuration. More particularly, when a bad sensors setting is considered, the cost function to be minimized in the TDOA localization inversion problem exhibits a much larger minimum zone (blue zone) leading to high biases in the estimation results.

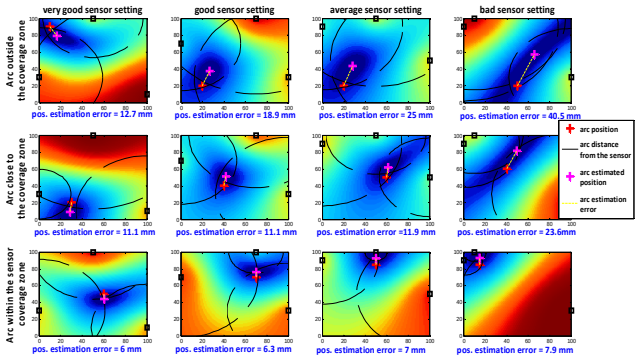

Figure 11: arc acoustic signal in the three sensors' timescale

Further on, the arc localization in a three dimensions volume has been simulated. A five acoustic sensors configuration has been evaluated on a 100 mm side cube arc localization problem. The same dependency of the dilution of precision on the coverage of the sensors is exhibited. The arc position estimation precision obtained by simulation spans from 2.3 mm, for the best sensor configuration, to 6.3 mm, for the worst sensors setting.

7 Demonstrator

A demonstrator (figure 12) has been realized in order to test our detector under conditions close to reality. The chosen geometry is consistent with those used in batteries developed at CEA. We have reproduced a typical assemblage of cylindrical cells using Plexiglas elements for safety reasons. Arcs are produced by melting a fuse wire on a PCB designed to create arcs of different amplitudes. It is also possible to replay the acoustic disturbances measured in the EV using ultrasound speakers. We put a microphone flush with the surface of the packaging. Acquisition is performed using National Instrument materials with a sampling frequency of 1 MHz. The detection by correlation described in this paper was implemented in Labview software.

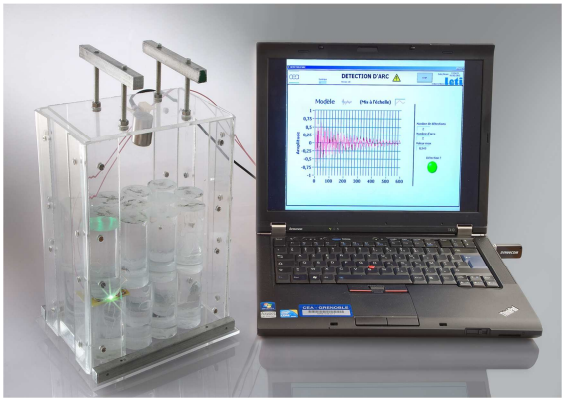

Figure 12: demonstrator with arcing flash present on a fuse wire placed between cylindrical cells in plexiglas and arc signal processing on the screen.

8 Conclusion

This study addressed different points: first of all, we have characterized the acoustic signature of an arc which gives us a fine knowledge of the signal to be detected. After this step, we studied the propagation of the waves in a battery so we identified how the acoustic signal arrives to the sensor. We have also inventoried many acoustic disturbances present in an EV in order to design the detector. One efficient arc detection method based on correlation has been studied. We have also developed a functional demonstrator that allowed us to validate our approach on safety conditions close to reality. Finally, an arc localization process have been simulated and analysed. Results show that fine localization accuracy can be reached even if the performances are related to the sensors configuration. Maintenance of the battery will be improved with this faulty connection localization.
This study has proven the feasibility of the arc detection and localization for a specific battery configuration.
The main perspective of the study is the development of a generic detection and localization system that can be adapted to any battery. As the geometry of the battery depends on the application, we must determine a law allowing the optimal deployment of the sensors into the battery. So we have to work on the model of acoustic propagation in other battery geometries. Finally, the final system aims to be embedded on battery with miniature and low cost sensors specific to the arc response. Technological developments are underway in CEA in this perspective. The miniaturization of the whole system and its integration within the battery will finally be the two key steps.

The authors thank Thibaut Journet and Cyrille Desmoulins from CEA and Cornel Ioana from GIPSA-Lab for their contribution to this work.

References

[1] S. Vacquié, *L'arc électrique*, Eyrolles, 2000

[2] P. Ravier, *Détection de transitoires par ondelettes adaptées*, thesis from EEATS, National Polytechnic Institute of Grenoble, 1998

[3] J.F. Sciabica, *Détection acoustique de larves xylophages dans le bois*, 10th French congress of acoustics, Lyon, April 2010

[4] V. Cattin, P. Perichon, J. Dahmani, *Detection of electric arcs in large batteries*, RITF congress, nov. 12-15, 2012

Authors

Viviane CATTIN
After an engineering degree in electronics and signal processing and a PhD in signal image and speech processing, I work at the CEA since 1998 as a research engineer in the fields of detection and localisation from magnetometers and accelerometers, as a leader of industrial and collaborative projects on motion capture and drift measurement of cars. I supervised two PhDs and several students on signal processing, recently applied to battery diagnosis and monitoring. I am currently in charge of a laboratory working on advanced electronics for energy and power applications.

Pierre PERICHON
After an engineering degree in electronics and computer engineering from Central Lille, I have worked for 17 years in Schneider Electric France on electronic breakers for low-voltage grid. Since 2005, I belong to the CEA organization and have worked for 5 years on photovoltaic systems (protection, power inverter, system…) and now on electrical cars. I am an expert in power electronics, electrical system and protections systems for DC and AC network (arc detector, breakers, ground fault protection…). I hold more than 30 patents.

Jawad DAHMANI
After an engineering degree in electronics from Polytech' Sophia Antipolis and a master in Mathematics applied to telecommunications, image and control signals, I led a research project in the CEA in the field signal processing for electrical arc detection.

Benjamin SCHWARTZMANN
After a dual engineering degree in electronics from Grenoble-INP and in electrical engineering from KTH Royal Institute of Technology, I have joined CEA in 2012 as a research engineer in the fields of signal processing, kalman filtering and optimization algorithms.

Vincent HEIRIES is graduated from ENAC (Ecole Nationale de l'Aviation Civile) and holds a PhD in signal processing and digital communications. He has worked several years in the field of navigation systems (GNSS, UWB). His activities in the CEA are now mainly focused on signal processing applied to battery monitoring.